https://doi.org/10.5194/egusphere-2026-609
Preprint. Discussion started: 16 February 2026

Measurement Report: Quantitative Analysis of Aerosol Acidity and Its Driving Factors in Guanzhong Area, Northwest China

Qian Wang[1,2], Xiao Guo[1], Minxia Shen[1], Yali Liu[3], Yifan Zhang[3], Lu Li[1], Weining Qi[1,2], Yue Cao[3], Shicong Li[1], Zhuoer Dong[1,2], Wenting Dai[1,4], Jianjun Li[1,4*]

[1]State Key Laboratory of Loess Science, Institute of Earth Environment, Chinese Academy of Sciences, Xi'an, 710061, China;

[2]University of Chinese Academy of Sciences, Beijing, China;

[3]Xi'an Institute for Innovative Earth Environment Research, Xi'an, China;

[4]National Observation and Research Station of Regional Ecological Environment Change and Comprehensive Management in the Guanzhong Plain, Xi'an, China;

Corresponding author: Jianjun Li, e-mail address:lijj@ieecas.cn

https://doi.org/10.5194/egusphere-2026-609
Preprint. Discussion started: 16 February 2026

Abstract. Aerosol acidity significantly affects atmospheric chemistry and human health, yet its driving factors remain controversial. This study systematically examined a year-long characteristics of water-soluble inorganic ions in $PM_{2.5}$ in the semi-arid Guanzhong Plain, Northwest China, and quantitatively analyzed its acidity and driving factors. The annual mean pH of $PM_{2.5}$ was 3.8 ± 1.0 (winter > spring > summer > autumn). As pollution increased, aerosol pH shifted from the acidic range (2-5) on clean days to a near-neutral range (3-6) on polluted days. Sensitivity tests and driver analysis revealed that atmospheric temperature (22.3%-33.8%), NH_x (gas NH_3+NH_4^+, 11.4%-44.9%), and SO_4^{2-} (8.5%-10.8%) were common key factors influencing pH across all seasons. Among these, temperature played a dominant role in seasonal variations, while NH_x was the primary contributor during autumn and winter. Notably, Ca^{2+} emerged as a unique driver specific to spring, the relative standard deviation (RSD) was 8.8%. Relative humidity (RH) exhibited a distinctive non-linear regulatory effect, i.e., aerosol pH initially decreases and subsequently increases with rising RH (inflection point occurred at 60%–85%). This phenomenon is primarily attributed to an abrupt change in liquid water content triggered by the deliquescence of hygroscopic components. Our results enhance the understanding of the contributions of various factors to aerosol pH and offers a new perspective for developing $PM_{2.5}$ control strategies in the semi-arid and ammonia-rich region.

Keywords: Aerosol acidity, aerosol liquid water, quantitative analysis, driving factors, Guanzhong Plain

https://doi.org/10.5194/egusphere-2026-609
Preprint. Discussion started: 16 February 2026

1. Introduction

Atmospheric aerosols play a vital role in the Earth's atmospheric system, significantly impacting regional and global air quality, climate change, and human health (Liu et al., 2025; Zhang et al., 2017). Among these properties, aerosol acidity, typically characterized by pH, is one of the most critical parameters. Research indicates that acidity can directly or indirectly regulate the gas-particle partitioning of semi-volatile species and the rates of chemical reactions (Guo et al., 2016; Paglione et al., 2021). It drives pH-dependent aqueous-phase reactions and impacts other processes related to particle formation and growth. Additionally, acidity can enhance the formation of secondary organic aerosol (SOA) and influence its transformation pathways through acid-catalyzed reactions (Rengarajan et al., 2011; Shi et al., 2019). Moreover, aerosol pH affects the dissolution of trace metals and the concentration of their toxic forms, with stronger acidity promoting metal dissolution via acid dissociation (Ding et al., 2019; Shi et al., 2011). High aerosol acidity levels have been linked to increased risks of respiratory illnesses and specific cancers. These acidity-driven atmospheric processes collectively contribute to the generation of intricate air pollution, the deposition of pollutants through dry and wet mechanisms, and their overall effects on human health and the climate system (Mao et al., 2009; Pye et al., 2020). Therefore, the exploration of particle pH is crucial for enhancing air quality management strategies and policy development, which is highly important for alleviating the health and environmental consequences of air pollution. The direct measurement of atmospheric aerosol acidity presents challenges (Xu et al., 2025), primarily due to the difficulties in quantifying the aqueous-phase concentrations of semi-volatile compounds and H^+ in ambient particulate matter. Thus, thermodynamic modellings, such as E-AIM (Clegg et al., 1998) and ISORROPIA (Nenes et al., 1998), were frequently used as a proxy method for assessing aerosol acidity in recent decades.

Aerosol acidity displays notable spatiotemporal variability, playing a crucial role in atmospheric environmental research. Globally, aerosols in Europe and North

https://doi.org/10.5194/egusphere-2026-609
Preprint. Discussion started: 16 February 2026

America generally exhibit higher acidity levels compared to those in China, with pH values 1–2 units lower (Zhang et al., 2021). In North America, coastal cities in Canada frequently exhibit greater aerosol acidity than inland regions, primarily due to elevated humidity that enhances the aqueous-phase oxidation of SO_2 (Brook et al., 1997). In China, aerosol acidity typically rises from north to south. Specifically, during winter in the heavily polluted North China Plain, pH values typically range from 4.1 to 4.9 (Ding et al., 2019; Liu et al., 2017; Shi et al., 2019; Tan et al., 2018). In the Guanzhong region, aerosol pH can reach as high as 5 (Wang et al., 2016). Conversely, coastal cities in southeastern China, such as Guangzhou and Xiamen, display significantly lower mean pH values of 2.5 and 3.5, respectively (Jia et al., 2020; Xu et al., 2025). Furthermore, vertical differences in aerosol acidity are also noteworthy. As altitude increases, aerosol acidity generally intensifies, with higher acidity observed at mountain summits compared to surface levels (Feng et al., 2023; Guo et al., 2016). Temporally, aerosol acidity is typically higher in summer than in winter, while patterns in spring and autumn fluctuate based on regional climatic and emission characteristics (Tan et al., 2018; Xu et al., 2025). In recent years, aerosol acidity has gained prominence in academic research and discussion due to its critical role in influencing aerosol physicochemical properties (Cui et al., 2025; Liu et al., 2021; Paglione et al., 2021; Tao et al., 2025). However, its levels are governed by numerous, complex, and region-dependent factors, leading to significant spatial heterogeneity. Therefore, investigating the dynamic changes in aerosol acidity throughout different seasons and understanding the underlying mechanisms are crucial for enhancing our comprehension of haze formation and developing precise air pollution control strategies.

Through quantitative analysis of aerosol pH driving factors and elucidation of $PM_{2.5}$ chemical composition and meteorological impacts across seasons, we can better understand spatiotemporal variation pattern (Jia et al., 2020; Xu et al., 2025). Previous studies showed that in Beijing, SO_4^{2-}, NH_x, and T significantly affect $PM_{2.5}$ pH, while Ca^{2+} and RH serve as dominant factors in spring and summer, respectively (Ding et al., 2019). In contrast, in southeastern Chinese cities such as Guangzhou and Xiamen,

https://doi.org/10.5194/egusphere-2026-609
Preprint. Discussion started: 16 February 2026

meteorological parameters like T and RH exert an even greater influence on pH variation than chemical components (Jia et al., 2020; Xu et al., 2025). These findings underscore the complexity of the factors influencing aerosol acidity. However, existing studies have largely focused on compositional analyses in specific cities, leaving our understanding of the trends in aerosol pH values and their primary drivers and relative contributions still insufficient. The discrepancies in conclusions from different research further highlight the geographical specificity of this issue.

Guanzhong Plain is a vital economic and agricultural center in northwestern China, the rapid industrial and urban development has resulted in severe air pollution complexities. The mechanisms of air pollution formation and its driving factors it in the region are significantly shaped by its inland geographical characteristics and socio-economic conditions. The unique semi-enclosed topography, with the Loess Plateau to the north and the Qinling Mountains to the south, restricts pollutant dispersion, leading to the accumulation of various pollutants and enabling complex chemical reactions (Huang et al., 2014; Liu et al., 2025; Shen et al., 2024). The area is known for its intensive agricultural practices, contributing to high levels of ammonia emissions that influence aerosol acid-base equilibrium. Additionally, long-distance transportation from the nearby Loess Plateau introduces alkaline mineral dust and crustal cations (e.g., Ca^{2+}, Mg^{2+}) that can neutralize acidic components effectively. Furthermore, distinct seasonal climates (e.g., stable conditions in winter, high temperatures in summer) further influence the transformation and removal processes of pollutants. The combination of these factors makes the Guanzhong Plain a unique location for a comprehensive study on aerosol pH trends and key influencing factors, which would differ from those in southeastern coastal cities of China, where marine air masses and hot, humid meteorological conditions predominantly influence air quality.

In this study, we conducted a year-long observation of water-soluble inorganic compositions of $PM_{2.5}$ in the Guanzhong region, and utilized an ISORROPIA-II model to access aerosol pH and liquid water content. It comprehensively examined the variations of these parameters throughout different seasons and under diverse

https://doi.org/10.5194/egusphere-2026-609
Preprint. Discussion started: 16 February 2026

pollution levels. Additionally, sensitivity tests and quantitative assessments were conducted to identify key factors influencing aerosol pH and to elucidate their relative contributions across seasons. This investigation establishes a robust scientific foundation for the implementation of precise ammonia emission reduction tactics, aiming to effectively decrease atmospheric fine particulate matter levels.

2. Materials and Methods

2.1 Sample collection

$PM_{2.5}$ samples were collected at the National Observation and Research Station of Regional Ecological Environment Change and Comprehensive Management in the Guangdong Plain, Shaanxi Province, China (34°3′39″N, 108°20′37″E; 503 m a.s.l.). This station is positioned at the northern foothills of the Qinling Mountains (Fig. 1) and functions as a regional background site. It is located approximately 60 km southwest of Xi'an city, with no significant industrial, traffic, or other substantial anthropogenic pollution sources. The sampling campaign spanned from January 1 to December 21, 2022, and a total of 295 valid samples were obtained during the study. Daily sampling was conducted from 10:00 to 09:00 the next day, lasting for 23 hours. Samples were collected using a medium-flow sampler (HC-1010, China Qingdao Company, China) equipped with quartz fiber filters (Whatman QMA, USA) with pre-baked (450 °C, 5 h) quartz fiber filters (Whatman, QMA, USA) at an airflow rate of 100 L min^{-1}. After sampling, each filter sample was promptly enveloped in aluminum foil, sealed, and frozen at -20°C for subsequent laboratory analysis. To ensure quality control, field blank samples were collected both before and after sampling. This involved placing pre-treated blank filters into the sampler, allowing them to stand for 10 minutes without activating the pump, and then sealing and storing them using the same procedure as the actual samples. The chemical analysis data for all samples were adjusted by deducting the average concentration measured from the two blank samples to eliminate potential systematic errors.

Daily average concentrations of PM_{10}, SO_2, NO_2, CO, and O_3-8h (defined as the maximum 8-hour average O_3 concentration) were obtained from the local government.

https://doi.org/10.5194/egusphere-2026-609
Preprint. Discussion started: 16 February 2026

Meteorological parameters, including ambient temperature (T), relative humidity (RH), wind speed (WS), and atmospheric pressure (AP), were acquired from the National Observation and Research Station for Regional Ecological Environment Change and Comprehensive Management in the Guanzhong Plain, Shaanxi Province, China.

2.2 Analysis of water-soluble inorganic ions and ammonium partitioning ratio

Water-soluble inorganic ions (WSIIs), including SO_4^{2-}, NO_3^-, NH_4^+, Cl^-, Ca^{2+}, K^+, Mg^{2+}, and Na^+, were analyzed using ion chromatography (Metrohm-940, Switzerland). To enhance measurement accuracy, a fixed amount of lithium bromide was added to the eluent. For quality assurance, one sample out of every ten was randomly selected for re-analysis. All WSII concentrations were corrected using field blanks, which exhibited concentrations less than 10% of those in ambient samples. The limits of detection (LODs) for SO_4^{2-}, NO_3^-, NH_4^+, Cl^-, Ca^{2+}, K^+, Mg^{2+}, and Na^+ were 0.027, 0.026, 0.0010, 0.0087, 0.0012, 0.0011, 0.0008, and 0.0005 μg m^{-3}, respectively (Liu et al., 2025). The mass concentrations of all detected WSIIs were significantly higher than their corresponding LODs.

As detailed in the preceding section, this study employed ammonium partitioning ratio (NHR) to quantify the transformation of gaseous ammonia into particulate ammonium (Xie et al., 2020; Zhang et al., 2021). This ratio is defined as the molar concentration of particulate ammonium ($n(NH_4^+)$, μmol m^{-3}) relative to the total molar concentration of inorganic ammonium ($n(NH_3) + n(NH_4^+)$, μmol m^{-3}), calculated using the following equation:

$$NHR = \frac{n(NH_4^+)}{n(NH_4^+) + n(NH_3)} \quad (1)$$

2.3 Calculation of aerosol pH

In this study, the ISORROPIA-II model was utilized to estimate aerosol thermodynamic parameters. The model was operated in "forward" mode, based on the assumption that aerosols were in a "metastable" state (Fountoukis et al., 2009; Nenes et al., 1998), with inputs including concentrations of SO_4^{2-}, NH_x, NO_3^-, Cl^-, Na^+, Ca^{2+}, K^+, Mg^{2+}, RH and T. Aerosol pH was calculated using the following equation:

https://doi.org/10.5194/egusphere-2026-609
Preprint. Discussion started: 16 February 2026

$$pH = -\lg\frac{1000\gamma_{H^+}H^+_{air}}{ALWC} \quad (2)$$

where γ_{H^+} is the hydronium ion activity coefficient (assumed = 1), H_{air}^+ (μg m^{-3}) indicates the concentration of hydronium ions per unit volume of air, and ALWC (μg m^{-3}) signifies the aerosol liquid water content. It should be noted that the model-calculated pH values are more reliable when the RH falls within the range of 30% to 95% (Guo et al., 2016)

Neglecting the influence of gaseous species, such as NH_3, HNO_3, and HCl, on aerosol acidity often results in an underestimation of acidity. The effect of these gases on aerosol pH can only be dismissed when their atmospheric concentrations are exceedingly low (Guo et al., 2015; Hennigan et al., 2015). In China, atmospheric ammonia concentrations are relatively high, and the study region is characterized by elevated ammonia levels; thus, NH_3 cannot be overlooked. The specific estimation method for NH_3 is outlined in Section 3.2. However, previous research has shown that the concentrations of gaseous HNO_3 and HCl in urban Xi'an remained below 1 μg m^{-3} throughout all seasons. Since the Qinling site serves as a background location, concentrations there are anticipated to be even lower. Given these negligibly low levels, we utilized the measured concentrations of particulate NO_3^- and Cl^- as inputs for TNO_3 and TCl, respectively (Nah et al., 2023).

2.4 Multiple linear regression model

In ammonia-rich regions, aerosol pH, particularly during winter, is primarily influenced by NH_3 levels (Tao and Murphy, 2019). However, the frequent absence of long-term and continuous NH_3 observational data impedes the analysis of long-term trends in $PM_{2.5}$ chemical properties. To fill this data gap and explore variations in aerosol pH in the research area, this study aimed to create a model for estimating the NHR based on easily accessible routine monitoring data to estimate NH_3 concentrations. Given the established relationships between NHR and factors such as NO_3^-, SO_4^{2-}, and T, we utilized multiple linear regression analysis with SPSS. This method identified species significantly correlated with NHR from the existing dataset and established quantitative relationships among them. Model parameters were estimated using the ordinary least squares method. Following model development, its

https://doi.org/10.5194/egusphere-2026-609
Preprint. Discussion started: 16 February 2026

validity and accuracy were rigorously assessed through a series of statistical methods, including the correlation coefficient, F-test, and t-test (Wei et al., 2023).

2.5 Sensitivity tests and quantitative analysis

This study assessed the impact of various factors on aerosol pH through sensitivity tests. The variables analyzed included meteorological parameters (T, RH) and chemical components (SO_4^{2-}, NH_x, NO_3^-, Cl^-, Na^+, Ca^{2+}, K^+, Mg^{2+}) (Tao and Murphy, 2019) The specific sensitivity analysis adhered to the methodology outlined by Ding et al. (2019): Within the ISORROPIA-II model, the measured value of a target variable i was used sequentially as input alongside the average values of all other parameters. By observing the resulting trend in the output pH, the individual effect of variable i on aerosol pH could be assessed.

Assuming the aerosol pH estimated under scenario 1 (pH_1) differed from that under scenario 2 (pH_2), the pH difference ($\Delta pH = pH_2 - pH_1$) was thus caused by the variations in the factors listed above. The quantitative analysis method adhered to the approach outlined by Zhou et al. (2022). To quantify the contribution of a single variable j within the ISORROPIA-II model, the value of factor j was altered from its Scenario 1 value to its Scenario 2 value, while all other parameters remained constant. The resulting change in pH was recorded as pH_j, which represents the independent contribution of that specific factor to the total ΔpH. The remaining change in pH, not accounted for by this procedure, is attributed to ΔpH_{others}, reflecting the combined effects of synergistic variations among the factors.

3. Results and discussion

3.1 Seasonal variations in $PM_{2.5}$ and its chemical composition

3.1.1 Seasonal variations in $PM_{2.5}$ and air pollutants

The annual variation for $PM_{2.5}$ mass concentrations, gaseous pollutants (SO_2, CO, NO_2, and O_3-8h), and meteorological parameters (T, RH, WS, and AP) are shown in Fig. 2, with seasonal statistics summarized in Table 1. The sampling period in 2022 was categorized into four seasons based on local heating patterns and human activity trends: winter (January 1 to March 12, and November 15 to December 21), spring (March 16 to May 31), summer (June 1 to August 30), and autumn (September 1 to

https://doi.org/10.5194/egusphere-2026-609
Preprint. Discussion started: 16 February 2026

November 14). During the observation period, the $PM_{2.5}$ mass concentration varied from 9.8 to 221.7 μg m^{-3}, with an annual mean of 65.3 ± 61.8 μg m^{-3}. This concentration is lower than those reported for other typical areas in the Guanzhong Plain (Liu et al., 2025; Zhang et al., 2019), aligning with expectations of minimal local emission influence at this site. In comparison to the annual mean of 105.6 μg m^{-3} recorded at a Qinling background station in 2012 (Niu et al., 2016), the concentration observed in this study is approximately 36% lower, suggesting a significant reduction in air pollution in recent years due to effective air quality control measures. $PM_{2.5}$ concentrations exhibited marked seasonal variations, showing the seasonal order of winter (93.5 ± 41.7 μg m^{-3}) > spring (61.4 ± 40.8 μg m^{-3}) > autumn (43.1 ± 25.1 μg m^{-3}) > summer (33.2 ± 13.7 μg m^{-3}). The majority of days exceeding the daily $PM_{2.5}$ limitation (Grade II, 75 μg m^{-3}) from the ambient air quality standards of China occurred in winter, with about 68% of daily average concentrations surpassing the limitation (Table S1). This trend underscores the significant influence of heating activities and adverse meteorological conditions on air quality.

The concentrations of gaseous pollutants also demonstrated significant seasonal variations. CO and NO_2, primary pollutants mainly from fossil fuel combustion, had higher levels in autumn and winter and lower levels in spring and summer, particularly elevated during the heating period compared to the non-heating period. This pattern is linked to increased emissions during heating demands in autumn and winter, along with unfavorable meteorological conditions hindering pollutant dispersion (Liu et al., 2025). Due to its strong dependence on solar radiation intensity and temperature, O_3-8h value peaked in July during summer (156.8 μg m^{-3}) and subsequently decreasing as sunlight weakened with varying intensity. This anti-phase variation underscores the seasonal differences in the dominant formation mechanisms for different pollutants.

3.1.2 Water-soluble inorganic ions in $PM_{2.5}$

The concentrations of WSIIs (SO_4^{2-}, NO_3^-, NH_4^+, Cl^-, Ca^{2+}, K^+, Mg^{2+}, Na^+) in $PM_{2.5}$ are shown in Fig. 1 and Table 1. The annual average concentration of total measured WSIIs was 24.5 ± 20.5 μg m^{-3}, representing approximately 38% of the

https://doi.org/10.5194/egusphere-2026-609
Preprint. Discussion started: 16 February 2026

$PM_{2.5}$ mass. Significant seasonal variations were noted, with concentrations following the order: winter (39.5 ± 22.0 μg m^{-3}) > autumn (19.8 ± 15.9 μg m^{-3}) > spring (18.6 ± 12.9 μg m^{-3}) > summer (8.5 ± 4.2 μg m^{-3}). Among the WSIIs, secondary inorganic aerosols (i.e., SO_4^{2-}, NO_3^-, and NH_4^+ (SNA)) were the predominant constituents, collectively contributing 89.0% to the total WSIIs. Notably, NO_3^- exhibited the highest concentration (8.8 μg m^{-3}, 35.9%), followed by SO_4^{2-} (5.1 μg m^{-3}, 20.7%) and NH_4^+ (4.0 μg m^{-3}, 16.3%), indicating nitrate as the most abundant ionic species. This might be due to driven by enhanced atmospheric oxidation and rising ammonia emissions via pathways like OH radical and N_2O_5 reactions. The ternary plot in Fig. S1 illustrates the molar concentration ratios of SO_4^{2-}, NO_3^-, and NH_4^+ across seasons. The proportion of NO_3^- within SNA was markedly greater in winter compared to summer, while the situation was reversed for SO_4^{2-}. These seasonal fluctuations primarily stem from the thermal instability and volatility of NH_4NO_3 at elevated T (Xu et al., 2025), the fractional contributions of NO_3^- reached minimum in summer. Simultaneously, heightened photochemical processes during summer promote the secondary production of SO_4^{2-}. Moreover, most data points cluster nearer to the NH_4^+ vertex. This directly indicates a relative abundance of atmospheric NH_3 during the observation period, adequate to neutralize the majority of sulfuric and nitric acids for ammonium salt formation. This constitutes direct chemical proof elucidating the relatively elevated aerosol pH levels in the ammonia-rich Guanzhong Plain region. The concributions of the remaining ions (Cl^-, K^+, Mg^{2+}, Ca^{2+}, Na^+) were relatively low, collectively constituting 12.6% of total WSIIs. Cl^- and K^+, commonly utilized as tracers for anthropogenic combustion, exhibited highest concentration in winter, likely linked to seasonal biomass burning in western and northern China and subsequent regional transport processes (M. Liu et al., 2025; Sun et al., 2013; Xie et al., 2020). These chemical characteristics, particularly the relative predominance of nitrate, reflect the evolution of $PM_{2.5}$ chemical properties influenced by China's air pollution control policies. Since the implementation of the Air Pollution Prevention and Control Action Plan in 2013, stringent industrial emission controls and coal reduction measures have yielded significant results, leading to a substantial decrease in SO_2

https://doi.org/10.5194/egusphere-2026-609
Preprint. Discussion started: 16 February 2026

concentrations. Su et al. (2024) reported that SO_2 concentrations in Xi'an decreased by approximately 79% from 2006 to 2021. This reduction has facilitated a shift in aerosol pollution type from sulfate-dominated to nitrate-dominated. This transformation in pollution type has emerged as a new characteristic of regional air pollution across China (Krotkov et al., 2016; Mao et al., 2022; Z. Wang et al., 2022).

Linear regression analysis (Fig. S2) revealed a significant correlation between the equivalent concentrations of cations and anions throughout all seasons. The annual average of the regression slope (AE/CE) was 0.92, indicating that $PM_{2.5}$ was generally weakly alkaline during the study period. This finding is consistent with other studies conducted in northern Chinese cities (Cao et al., 2013; Shi et al., 2017), yet it contrasts with historical records indicating near-neutral to slightly acidic aerosols in Xi'an in 2005 and Beijing in 2014 (Tan et al., 2018; Shen et al., 2007). The alteration in acid-base characteristics is a result of reduced sulfur emissions due to China's air pollution control efforts, impacting the chemical composition of $PM_{2.5}$. This transformation corresponds with findings in Southwestern China from 2012 to 2016 (Chen et al., 2017, 2019; Huang et al., 2022). Seasonally, the AE/CE ratios for all seasons in 2022 remained below 1. The lowest ratios occurred in spring (0.88) and summer (0.89), which may be associated with the frequent dust events during these seasons that introduce more alkaline dust particles. It is noteworthy that the measurement methods used in this study did not include $CO_3^{2-}$and HCO_3^-, which are significant contributors to the anion deficit.

The linear relationship between the observed and predicted NH_4^+, based on local ammonia availability, is depicted in Fig. S3. When assuming that NO_3^- and SO_4^{2-} exist in the forms of $(NH_4)_2SO_4$ and NH_4NO_3, the slope (k) for each season approaches 1, indicating complete conversion to $(NH_4)_2SO_4$. NH_4^+ first reacts with SO_4^{2-} to form $(NH_4)_2SO_4$. After SO_4^{2-} is completely neutralized, any excess NH_4^+ then reacts with NO_3^- to form NH_4NO_3. The $k < 1$ signifies NH_4^+ excess post-reaction with SO_4^{2-} and NO_3^-. In practice, the observed excess NH_4^+ may interact with other anions, such as Cl^- from biomass burning, potentially forming NH_4Cl.

3.2 Establishment and validation of NH_3 concentration calculation methods

https://doi.org/10.5194/egusphere-2026-609
Preprint. Discussion started: 16 February 2026

NH_3 emissions significantly impact atmospheric chemical processes and act as a crucial precursor for the formation of secondary particulate matter (Liu et al., 2019; Saraswati et al., 2019). The multiphase buffer theory clarifies that the NH_3/NH_4^+ conjugate pair core buffering system regulates aerosol acidity (Zheng et al., 2020). Guanzhong Plain as a typical ammonia-rich region, elevated NH_3 emissions not only suggest an increased potential for secondary aerosol formation but also indicate that aerosol acidity is subject to robust internal buffering regulation (Zhang et al., 2021; Zheng et al., 2023). However, the lack of online monitoring data for gaseous NH_3 at the sampling site limits the accuracy of pH estimation using thermodynamic models. Therefore, it is important to establish a reliable method for estimating NH_3. In this study, we adapted the methodology of Wei et al. (2023), with the researchers using multiple linear regression analysis, to estimate the NHR relying on our previous short-term scale datasets (Wu et al., 2020). This is because the direct estimation of NH_3 is prone to interference from meteorological factors and the gas-particle distribution of acidic precursors, resulting in unstable outcomes. Consequently, this study opts to estimate NH_3 through NHR and assesses the method's accuracy (Meng et al., 2018; Wei et al., 2023).

Table 2 and S2 summarize the total results of multiple linear regression analysis in each season. The F-test and t-test results reveal significant correlations for all seasons ($R > 0.82$, $P < 0.01$), confirming the efficacy of the established statistical regression equations. Subsequently, a Pearson correlation analysis was performed to elucidate the statistical associations between NHR and diverse environmental factors. As shown in Fig. 3 and Table S3, NHR exhibited significant correlations ($P < 0.01$) with all selected environmental factors in both winter and spring. Among these, the highest correlation coefficient was observed between NO_3^- and SO_4^{2-} ($R = 0.96$, $P < 0.01$). Across all four seasons, NHR showed good correlations with either NO_3^- or SO_4^{2-}, but with distinct seasonal variations. In winter and spring, NHR displayed the highest Pearson correlation coefficients with NO_3^- ($R = 0.86$, $P < 0.01$ in winter; $R = 0.74$, $P < 0.01$ in spring). Conversely, in summer and autumn, NHR correlated most significantly with SO_4^{2-} ($R = 0.75$, $P < 0.01$ in summer; $R = 0.79$, $P < 0.01$ in autumn).

https://doi.org/10.5194/egusphere-2026-609
Preprint. Discussion started: 16 February 2026

These seasonal distinctions primarily arise from fluctuations in the thermodynamic stability of different ammonium salts and the seasonal alterations in their formation pathways (Tao et al., 2025; Zhang et al., 2021).

We also accessed the reliability of MRL model results by comparing the estimated NHR with the observed NHR in 2016 and 2017. The validation results (Fig. 4) indicated significant correlations across all seasons (with the intercept constrained to zero, all $R^2 > 0.94$, $P < 0.01$). Thus, the NH_3 concentrations in this study could be subsequently determined by inversely calculating the estimated NHR. Finally, these NH_3 values, along with the measured NH_4^+ data, were incorporated into the ISORROPIA-II model to simulate aerosol pH (refer to Section 3.3 for further details).

3.3 Seasonal variation in aerosol pH and pH under different pollution levels

Figure 5 shows the monthly averages of aerosol pH, aerosol liquid water content (ALWC), and H_{air}^+, as calculated by the ISORROPIA-II model during the 2022 sampling period. The annual average aerosol pH at the Qinling observation site was 3.8 ± 1.0. The seasonal pH averages ranked as follows: winter (4.9 ± 0.4) > spring (3.4 ± 0.7) > autumn (3.2 ± 0.7) > summer (2.8 ± 0.7). The average ALWC concentration was 60.3 μg m^{-3}, exhibiting the pattern: winter (80.4 ± 112.9 μg m^{-3}) > autumn (76.2 ± 121.0 μg m^{-3}) > spring (55.7 ± 132.2 μg m^{-3}) > summer (10.0 ± 25.1 μg m^{-3}). Overall, aerosol pH was highest in winter and lowest in summer, with spring and autumn values intermediate. This trend closely aligns with the seasonal evolution of $PM_{2.5}$ chemical composition and meteorological conditions, reflecting the seasonal pH variation pattern observed in Beijing (Ding et al., 2019). Winter aerosol pH was similar to those reported in Xi'an previously and slightly higher than those recorded during the COVID-19 period (Liu et al., 2025). A comparison of aerosol acidity levels across various regions in China is detailed in Table S4, revealing substantial regional variability. In contrast to southeastern coastal cities such as Shanghai and Xiamen, typical inland cities like Xi'an and Beijing generally display higher aerosol pH (Fu, 2022; Liu et al., 2025; Xu et al., 2025).

To further explore the seasonal characteristics in $PM_{2.5}$ acidity/alkalinity under different pollution levels, this study classified $PM_{2.5}$ mass concentrations into two

https://doi.org/10.5194/egusphere-2026-609
Preprint. Discussion started: 16 February 2026

categories based on ambient air quality standards of China: clean days (< 75 μg m^{-3}) and polluted days (> 75 μg m^{-3}). A systematic comparison of aerosol pH and ALWC variations corresponding to these pollution levels across different seasons was performed (Table S5). Under clean conditions, aerosol pH ranged from 2 to 5, whereas under polluted and heavily polluted conditions, it was primarily concentrated between 3 and 6. As air quality declined and $PM_{2.5}$ concentrations increased from clean to polluted days, the concentrations of aerosol components and pH values exhibited an upward trend across all seasons. However, the behaviors of RH, ALWC, and H_{air}^+ displayed seasonal discrepancies. In spring and summer, RH, ALWC, and H_{air}^+ decreased as $PM_{2.5}$ concentrations increased. Conversely, during autumn and winter, these parameters increased alongside rising $PM_{2.5}$ concentrations. These findings reveal fundamental differences in the dominant chemical mechanisms of $PM_{2.5}$ pollution formation across seasons.

During spring and summer, pollution formation is mainly controlled by gas-phase photochemical oxidation (Chen et al., 2025; Li et al., 2021). The enhanced solar radiation and high temperatures during these seasons collectively create a highly oxidizing atmospheric environment. While promoting the transformation of precursors, these conditions also drive the decomposition of semi-volatile NH_4NO_3, leading to the release of gaseous HNO_3 and NH_3 (Guo et al., 2018; Tao et al., 2025). Consequently, despite an increase in $PM_{2.5}$ concentrations, both ALWC and H_{air}^+ concentrations exhibit a decreasing or stabilizing trend due to the reduction of hygroscopic nitrate, while RH remains relatively low because of higher T. In contrast, autumn and winter are characterized by pollution processes driven by heterogeneous and aqueous-phase chemical reactions. The cold temperatures and stagnant weather conditions lead to high RH, promoting the aqueous-phase oxidation of pollutants and inhibiting the evaporation of NH_4NO_3 (Wang et al., 2016; Zhang et al., 2021). This results in the significant formation of highly hygroscopic NH_4NO_3 and $(NH_4)_2SO_4$, which triggers an increase in ALWC. This increase further intensifies heterogeneous reactions and concentrates acidic products, leading to a concurrent rise in H_{air}^+ concentration. Consequently, a complex pollution scenario emerges, characterized by

https://doi.org/10.5194/egusphere-2026-609
Preprint. Discussion started: 16 February 2026

a simultaneous increase in $PM_{2.5}$ ALWC, and H_{air}^+ concentrations.

3.4 Sensitivity analysis for aerosol pH

Sensitivity analysis of aerosol pH and ALWC in response to meteorological conditions and chemical composition is a crucial step for understanding and predicting atmospheric environmental changes. This analysis not only clarifies the nonlinear processes involved in secondary aerosol formation but also assesses the impact of variations in anthropogenic emissions on atmospheric chemical systems (Nah et al., 2023; Zhou et al., 2022). In this study, sensitivity analyses were performed for each season, incorporating both particulate-phase compositions and meteorological factors. The effects of SO_4^{2-}, NO_3^-, NH_x (gas NH_3 + NH_4^+), Cl^-, Ca^{2+}, K^+, Mg^{2+}, RH, and T on aerosol pH, ALWC, and H_{air}^+ were evaluated, as illustrated in Fig. 6. The primary drivers influencing aerosol pH variation across all seasons were NH_x, SO_4^{2-}, and T, while Ca^{2+} in spring and RH in summer also emerged as important influencing factors. This pattern is consistent with the drivers identified in the Beijing area (Ding et al., 2019). Regarding ALWC, RH emerged as the most significant factor, followed by NO_3^- and SO_4^{2-}.

Sulfate as a key component of secondary inorganic aerosols, is one of the most significant acidic sources in atmospheric fine particulate matter. Sulfuric acid, generated through heterogeneous oxidation processes, is a strong acid that directly increases the concentration of H_{air}^+ in the particulate phase and reduces the pH (Shah et al., 2018; Zhang et al., 2021). As illustrated in Fig. 6, when the levels of alkaline substances such as NH_3 are maintained constant, aerosol pH significantly declines with increasing SO_4^{2-} concentration. The concurrent rise in ALWC and H_{air}^+ further substantiates its direct role in driving acidification processes (Ding et al., 2019). The increase in ALWC and H_{air}^+ is particularly pronounced during summer and autumn. This sustained rise continuously depletes alkaline buffering substances in the particulate phase, resulting in heightened hydrogen ion activity and increased acidity (Guo et al., 2018). Conversely, while nitrate similarly elevates H_{air}^+ and ALWC, its overall impact on pH is generally weaker than that of sulfate due to its high volatility (Ding et al., 2019). Except during summer when the pH remained relatively stable,

https://doi.org/10.5194/egusphere-2026-609
Preprint. Discussion started: 16 February 2026

pH values decreased with rising NO_3^- concentrations in all other seasons.

Ammonia (NH_3), the primary alkaline gas, plays a crucial role in buffering aerosol pH. In ammonia-rich environments, NH_3 effectively counteracts acidic components, stabilizing pH and resulting in a nonlinear pH response to precursor concentrations (Cui et al., 2025; Karydis et al., 2021; Niu et al., 2016). Simultaneously, the dissolution of NH_3 into the particle phase to form NH_4^+ markedly enhances the hygroscopicity of particles, causing an increase in ALWC as NH_x concentrations rise (Jia et al., 2020; Liu et al., 2019). Studies indicate that NH_3 first reacts with H_2SO_4 and subsequently with HNO_3 to form NH_4NO_3. After most nitrate is converted to NH_4NO_3, it becomes difficult to dissolve additional NH_3 into aerosol droplets (Ding et al., 2019; Xu et al., 2025). The results of this study (Fig. 6) show that the response of pH to NH_x is non-linear. When the NH_x mass concentration is within the range of 3–10 μg m^{-3}, aerosol pH increases significantly, H_{air}^+ decreases sharply, and ALWC increases with rising NH_x concentration. Nevertheless, when the NH_x concentration surpasses a specific threshold, the trends in pH and H_{air}^+ decelerate and subsequently remain relatively stable. It should be noted that the results may be less accurate when NH_x concentration is below 3 μg m^{-3}, as high temperature and intense solar radiation promote the thermal decomposition of semi-volatile ammonium salts. The seasonal variations observed in this study further substantiate the regulatory role of atmospheric ammonia.

Ca^{2+} is an important crustal element in mineral dust, displaying distinct regional chemical characteristics and effects on aerosol acidity. According to the ISORROPIA-II model, Ca^{2+} typically combines with SO_4^{2-} to form the less soluble $CaSO_4$ solid phase, reducing its solubility and diminishing its effectiveness for neutralizing atmospheric acidity (Fountoukis et al., 2007; G. Wang et al., 2016). In the Guanzhong Plain, the regulatory impact of Ca^{2+} on aerosol pH is particularly crucial, especially due to the region's proximity to the Loess Plateau and its semi-arid climate. Dust transport from the northwest could shape the alkaline atmospheric conditions in this area. This phenomenon results in neutral aerosol pH in the free troposphere and contributes to the alkalinity of cloud water at high-altitude sites(Liu et al., 2024; Shen

https://doi.org/10.5194/egusphere-2026-609
Preprint. Discussion started: 16 February 2026

et al., 2024). Elevated concentrations of Ca^{2+} can increase aerosol pH by decreasing both ALWC and H_{air}^{+}, with the most pronounced impact observed during the frequent dust events of spring. These events transport significant amounts of alkaline mineral dust, enhancing acid neutralization, consistent with studies in northern China (Shi et al., 2019; Tan et al., 2018). This study revealed that the relative standard deviation (RSD) for Ca^{2+} concentration variation in spring reached 8.8%, notably higher than the corresponding RSD of 7.5% reported for the North China Plain during the same season(Ding et al., 2019). Conversely, in southern coastal urban areas like Xiamen and Guangzhou, which lack robust dust origins, the impact of Ca^{2+} on aerosol pH is typically negligible (Jia et al., 2020; Xu et al., 2025).This finding directly confirms the greater influence of dust sources in the Guanzhong Plain.

In addition to the particulate chemical composition, meteorological conditions, specifically RH and T, significantly influence aerosol acidity. This study revealed that during winter, spring, and autumn, aerosol pH displayed a non-linear response to increasing RH, characterized by an initial decrease followed by a subsequent increase. The inflection point typically occurred within the RH range of 60%–85%. Beyond this critical threshold, ALWC entered a phase of exponential growth. This phenomenon is probably driven by the deliquescence of the predominant hygroscopic components within the aerosol, primarily NH_4NO_3 and $(NH_4)_2SO_4$, which have deliquescence relative humidities of approximately 62% and 80% (Tang, 1996). Given that actual atmospheric particles are mixtures of various components, their hygroscopic and phase-state characteristics are more complicated (Su et al., 2022; Zheng et al., 2020). In the initial stage, an increase in RH results in a higher ALWC, which facilitates the heterogeneous uptake and aqueous-phase oxidation of acidic precursors, resulting in the formation of strong acids. During this phase, the acid-forming effect dominates the pH change (Du et al., 2020; Zhang et al., 2021). Once RH exceeds a critical threshold, ALWC exhibits an exponential growth trend. At this point, the intense dilution effect of RH on H^{+} begins to surpass the ongoing acid-forming effect (Karydis et al., 2021). Furthermore, this hygroscopic growth is self-reinforcing, i.e. the increased ALWC provides a more extensive aqueous medium

https://doi.org/10.5194/egusphere-2026-609
Preprint. Discussion started: 16 February 2026

for heterogeneous reactions of gaseous precursors, leading to further formation of hygroscopic salts and further promoting ALWC growth, and thus establishing a positive feedback loop (Su et al., 2022). Concurrently, under high RH conditions, thermodynamic factors favor the partitioning of semi-volatile ammonium salts into the particle phase. This neutralization process further depletes H^+ (Tao et al., 2025). These combined effects ultimately lead to the observed recovery in pH. Ambient temperature can influence aerosol pH by affecting gas-particle partitioning (Ding et al., 2019). The evaporation of semi-volatile ammonium salts plays a crucial role in aerosol acidification by transferring H^+ to the particle phase, consequently decreasing pH (Guo et al., 2018). Elevated ambient temperatures intensify this acidification mechanism synergistically. Thermodynamically, elevated temperatures drive the volatilization process. Concurrently, they reduce ALWC to concentrate H^+ and further enhancing acidity.

3.5 Quantitative analysis of pH driving factors

To quantitatively analyze aerosol pH, the contributions of various influencing factors to aerosol pH and ALWC were further quantified (Fig. 7 and Fig. S4). According to the multiphase buffer theory (Zheng et al., 2020), T significantly drives the seasonal variation of aerosol pH by influencing pKa*. The results presented in Fig. 7 confirm this assertion, indicating that T plays a dominant role (22.3%–31.6%) in driving the seasonal variation of aerosol pH. T favored enhanced aerosol acidity in winter and spring, while the opposite trend was observed in summer and autumn. Moreover, NH_x emerged as a key factor influencing aerosol pH during winter and autumn, contributing between 22.9% and 44.9%. When the higher winter NH_x concentration was replaced with the lower concentration observed in spring, while maintaining other winter parameters constant, the simulated ΔpH was negative, indicating increased acidity. In the winter, the widespread use of coal for heating leads to significant emissions of acidic gases (Wang et al., 2016). The decrease in concentrations may exacerbate acidification through two mechanisms. On one hand, it weakens the basic buffering capacity driven by NH_3, reducing its neutralizing effect on sulfuric and nitric acids. On the other hand, it disrupts the gas-particle equilibrium

https://doi.org/10.5194/egusphere-2026-609
Preprint. Discussion started: 16 February 2026

of NH_4NO_3, driving the equilibrium towards dissociation and resulting in the production of more gaseous HNO_3. These two processes together contribute to a decline in system pH. In contrast, the opposite trend is observed in the autumn. The primary influencing factors in spring were T at 31.9% and NVCs at 24.7%, while in summer, they were T at 33.8% and RH at 17.8%. These results suggest that NVCs, including Ca^{2+}, serve as significant drivers of aerosol pH variation in spring, while RH plays a similar role in summer. This observation is consistent with findings from studies conducted in other northern Chinese cities (Ding et al., 2019). Moreover, the synergistic effects of various influencing factors leading to ΔpH_{others} are also significant, particularly in autumn, where they contributed 26.6% to aerosol pH variation.

Throughout the observation period, chemical components contributed an average of 47.7% annually to pH, while meteorological factors contributed 35.7%, highlighting the greater impact of chemical components over meteorological factors. This characteristic significantly differs from that observed in southeastern coastal regions of China. For example, studies conducted in Xiamen and Guangzhou have demonstrated that the contribution of meteorological factors frequently surpasses that of chemical components (Jia et al., 2020; Xu et al., 2025). Seasonally, chemical components were more influential in winter (58.7%), spring (42.7%), and autumn (49.2%). Conversely, meteorological factors displayed their most significant impact in summer, with a contribution rate reaching 51.6%, thus serving as the primary driver of pH variation during this season.

4 Conclusions

This study evaluates the aerosol acidity across four seasons in the Guanzhong region of China and quantitatively analyzes the factors contributing to seasonal pH variations. Over the study period, $PM_{2.5}$ in the study area was generally weakly alkaline, with an annual mean aerosol pH of 3.8 ± 1.0. This trend corresponds with the seasonal changes in $PM_{2.5}$ chemical composition and meteorological conditions. Aerosol pH increased alongside rising $PM_{2.5}$ concentrations, ranging from 2–5

https://doi.org/10.5194/egusphere-2026-609
Preprint. Discussion started: 16 February 2026

(average: 3.4 ± 0.9) on clean days to 3–6 (4.8 ± 0.5) on polluted and heavily polluted days. Sensitivity analysis and quantitative analysis indicated that NH_x, SO_4^{2-}, RH, and T are key drivers driving pH across all seasons. T emerged as the primary driver of seasonal pH fluctuations (contributing 22.3%–31.6%), with NH_x playing a significant role in autumn and winter (contributing 22.9%–44.9%), while Ca^{2+} in spring and RH in summer acted as specific drivers for those seasons. pH showed higher sensitivity to SO_4^{2-} than to NO_3^-. Furthermore, NH_x not only displayed substantial buffering capacity on pH but also, upon conversion to NH_4^+ in the particle phase, enhanced particle hygroscopicity, resulting in increased ALWC with higher NH_x concentrations. Meteorological conditions, beyond chemical components, exerted a non-linear regulatory influence on acidity. During winter, spring, and autumn, aerosol pH initially decreases and subsequently increases with rising RH, exhibiting an inflection point within the RH range of 60%–85%. This behavior might be related to the explosive growth in ALWC that occurs when the predominant hygroscopic components, primarily NH_4NO_3 and $(NH_4)_2SO_4$, reach their mixed deliquescence point. Our results discovered the main driving factors of aerosol acidity and alkalinity in the Guanzhong Plain, which would be helpful for deeply understanding the heterogenous formation of atmospheric secondary aerosols in the semi-arid region.

Data availability

The data in this study are available at https://zenodo.org/records/18455742 (Wang et al., 2026).

Author contributions

Jianjun Li conceived and designed the study, and the revision of the manuscript. Qian Wang conducted the literature search, performed sample and data analysis, and wrote the manuscript. Xiao Guo, Minxia Shen, Yali Liu, Yifan Zhang, Lu Li, Weining Qi, Yue Cao, Shicong Li, Zhuoer Dong and Wenting Dai collected particulate samples and supervised the experiments. All authors provided critical feedback on the manuscript and approved the final version.

Conflict of Interest

https://doi.org/10.5194/egusphere-2026-609
Preprint. Discussion started: 16 February 2026

The authors declare no conflicts of interest relevant to this study.

Acknowledgments

This work was supported by the program from National Natural Science Foundation of China (No. 42577120)， the Natural Science Basic Research Program of Shaanxi (2025JC-YBQN-450) and the National Natural Science Foundation of China (No. 42407156). Jianjun Li also acknowledged the support of the Youth Innovation Promotion Association Chinese Academy of Sciences.

https://doi.org/10.5194/egusphere-2026-609
Preprint. Discussion started: 16 February 2026

References

Brook, R., Wiebe, A. H., Woodhouse, A., Audette, V., Piechowski, M., Dabek-Zlotorzynska, E., and Dloughy, F.: Temporal and spatial relationships in fine particle strong acidity, sulphate, PM_{10}, and $PM_{2.5}$ across multiple Canadian locations. Atmos. Environ., 31, 4223–4236. https://doi.org/10.1016/S1352-2310(97)00248-3, 1997.

Cao, J., Tie, X., Dabberdt, W. F., Jie, T., Zhao, Z., An, Z., Shen, Z., and Feng, Y.: On the potential high acid deposition in northeastern China. J. Geophys. Res.: Atmos., 118, 4834–4846. https://doi.org/10.1002/jgrd.50381, 2013.

Chen, G., Fan, X., Lin, Z., Ji, X., Chen, Z., Xu, L., and Chen, J.: Driving factors and photochemical impacts of Cl_2 in coastal atmosphere of southeast China. npj Clim. Atmos. Sci., 8, 135, https://doi.org/10.1038/s41612-025-01022-y, 2025.

Chen, Y., Xie, S., Luo, B., and Zhai, C.: Particulate pollution in urban chongqing of southwest China: historical trends of variation, chemical characteristics and source apportionment. Sci. Total Environ., 584–585, 523–534, https://doi.org/10.1016/j.scitotenv.2017.01.060, 2017.

Chen, Y., Xie, S., Luo, B., and Zhai, C.: Characteristics and sources of water-soluble ions in $PM_{2.5}$ in the Sichuan basin, China. Atmosphere, 10(78), https://doi.org/10.3390/atmos10020078, 2019.

Clegg, S. L., Brimblecombe, P., and Wexler, A. S.: Thermodynamic model of the system H^+-NH_4^+-Na^+-SO_4^{2-}-NO_3^--Cl^--H_2O at 298.15 K. J. Phys. Chem. A, 102, 2155–2171, https://doi.org/10.1021/jp973043j, 1998.

Cui, H., Du, Y., Zhang, H., Deng, M., Zhang, Q., Chen, W., Su, S., Li, X., Sarkar, S., Yang, L., Wang, X., and Jia, S.: A quantitative study on the influencing pathways of aerosol acidity: the non-neglectable role of non-ideality. Atmos. Environ., 354, 121256, https://doi.org/10.1016/j.atmosenv.2025.121256, 2025.

Ding, J., Zhao, P., Su, J., Dong, Q., Du, X., and Zhang, Y.: Aerosol pH and its driving factors in Beijing, Atmos. Chem. Phys., 19(12), 7939–7954, https://doi.org/10.5194/acp-19-7939-2019, 2019.

Du, C., Yang, H., Wang, N., Pang, S., and Zhang, Y.: pH effect on the release of NH_3 from

https://doi.org/10.5194/egusphere-2026-609
Preprint. Discussion started: 16 February 2026

639 the internally mixed sodium succinate and ammonium sulfate aerosols. Atmos. Environ., 220,
640 117101, https://doi.org/10.1016/j.atmosenv.2019.117101, 2020.
641 Feng, Q., Liu, H., Dai, W., Cao, Y., Shen, M., Liu, Y., Qi, W., Chen, Y., Guo, X., Zhang, Y.,
642 Li, L., Zhou, B., and Li, J.: Comparison of chemical composition and acidity of size-resolved
643 inorganic aerosols at the top and foot of mt. Hua, northwest China: the role of the gas-particle
644 distribution of ammonia. Sci. Total Environ., 905, 166985,
645 https://doi.org/10.1016/j.scitotenv.2023.166985, 2023.
646 Fu, Z., Cheng, L., Ye, X., Ma, Z., Wang, R., Duan, Y., Tao, J., and Cheng, J.: Characteristics
647 of aerosol chemistry and acidity in shanghai after $PM_{2.5}$ satisfied national guideline: Insight
648 into future emission control. Sci. Total Environ., 827, 154319,
649 http://dx.doi.org/10.1016/j.scitotenv.2022.154319, 2022.
650 Guo, H., Xu, L., Bougiatioti, A., Cerully, K. M., Capps, S. L., Hite, J. R., Carlton, A. G., Lee,
651 S.-H., Bergin, M. H., Ng, N. L., Nenes, A., and Weber, R. J.: Fine-particle water and pH in
652 the southeastern united states. Atmos. Chem. Phys., 15(9), 5211–5228,
653 https://doi.org/10.5194/acp-15-5211-2015, 2015.
654 Guo, H., Sullivan, A. P., Campuzano-Jost, P., Schroder, J. C., Lopez-Hilfiker, F. D., Dibb, J.
655 E., Jimenez, J. L., Thornton, J. A., Brown, S. S., Nenes, A., and Weber, R. J.: Fine particle pH
656 and the partitioning of nitric acid during winter in the northeastern united states. J. Geophys.
657 Res.: Atmos., 121(17), https://doi.org/10.1002/2016JD025311, 2016.
658 Guo, H., Otjes, R., Schlag, P., Kiendler-Scharr, A., Nenes, A., and Weber, R. J.: Effectiveness
659 of ammonia reduction on control of fine particle nitrate. Atmos. Chem. Phys., 18(16),
660 12241–12256, https://doi.org/10.5194/acp-18-12241-2018, 2018.
661 Hennigan, C. J., Izumi, J., Sullivan, A. P., Weber, R. J., and Nenes, A.: A critical evaluation
662 of proxy methods used to estimate the acidity of atmospheric particles, Atmos. Chem. Phys.,
663 15(5), 2775–2790, https://doi.org/10.5194/acp-15-2775-2015, 2015.
664 Huang, R., Zhang, Y., Bozzetti, C., Ho, K., Cao, J., Han, Y., Daellenbach, K. R., Slowik, J.
665 G., Platt, S. M., Canonaco, F., Zotter, P., Wolf, R., Pieber, S. M., Bruns, E. A., Crippa, M.,
666 Ciarelli, G., Piazzalunga, A., Schwikowski, M., Abbaszade, G., Schnelle-Kreis, J.,
667 Zimmermann, R., An, Z., Szidat, S., Baltensperger, U., Haddad, I. E., and Prévôt, A. S. H.:
668 High secondary aerosol contribution to particulate pollution during haze events in China.

https://doi.org/10.5194/egusphere-2026-609
Preprint. Discussion started: 16 February 2026

669 Nature, 514(7521), 218–222, https://doi.org/10.1038/nature13774, 2014.
670 Huang, Y., Zhang, L., Peng, C., Chen, Y., Li, T., and Yang, F.: Pollution characteristics of
671 water-soluble inorganic ions in $PM_{2.5}$ from a mountainous city in southwest China.
672 Atmosphere, 13(10), 1713, https://doi.org/10.3390/atmos13101713, 2022.
673 Jia, S., Chen, W., Zhang, Q., Krishnan, P., Mao, J., Zhong, B., Huang, M., Fan, Q., Zhang, J.,
674 Chang, M., Yang, L., and Wang, X.: A quantitative analysis of the driving factors affecting
675 seasonal variation of aerosol pH in Guangzhou, China. Sci. Total Environ., 725, 138228,
676 https://doi.org/10.1016/j.scitotenv.2020.138228, 2020.
677 Karydis, V. A., Tsimpidi, A. P., Pozzer, A., and Lelieveld, J.: How alkaline compounds
678 control atmospheric aerosol particle acidity. Atmos. Chem. Phys., 21(19), 14983–15001,
679 https://doi.org/10.5194/acp-21-14983-2021, 2021.
680 Krotkov, N. A., McLinden, C. A., Li, C., Lamsal, L. N., Celarier, E. A., Marchenko, S. V.,
681 Swartz, W. H., Bucsela, E. J., Joiner, J., Duncan, B. N., Boersma, K. F., Veefkind, J. P.,
682 Levelt, P. F., Fioletov, V. E., Dickerson, R. R., He, H., Lu, Z., and Streets, D. G.: Aura OMI
683 observations of regional SO_2 and NO_2 pollution changes from 2005 to 2015. Atmos. Chem.
684 Phys., 16(7), 4605–4629, https://doi.org/10.5194/acp-16-4605-2016, 2016.
685 Li, K., Jacob, D. J., Liao, H., Qiu, Y., Shen, L., Zhai, S., Bates, K. H., Sulprizio, M. P., Song,
686 S., Lu, X., Zhang, Q., Zheng, B., Zhang, Y., Zhang, J., Lee, H. C., and Kuk, S. K.: Ozone
687 pollution in the north China plain spreading into the late-winter haze season. Proc. Natl. Acad.
688 Sci., 118(10), e2015797118, https://doi.org/10.1073/pnas.2015797118, 2021.
689 Liu, H., Feng, Q., Huang, Y., Wu, F., Liu, Y., Shen, M., Guo, X., Dai, W., Qi, W., Zhang, Y.,
690 Li, L., Wang, Q., Zhou, B., and Li, J.: Composition and size distribution of wintertime
691 inorganic aerosols at ground and alpine regions of northwest China. Chin. Chem. Lett., 35(11),
692 109636, https://doi.org/10.1016/j.cclet.2024.109636, 2024.
693 Liu, M., Song, Y., Zhou, T., Xu, Z., Yan, C., Zheng, M., Wu, Z., Hu, M., Wu, Y., and Zhu, T.:
694 Fine particle pH during severe haze episodes in northern China. Geophys. Res. Lett., 44(10),
695 5213–5221, https://doi.org/10.1002/2017GL073210, 2017.
696 Liu, M., Huang, X., Song, Y., Tang, J., Cao, J., Zhang, X., Zhang, Q., Wang, S., Xu, T., Kang,
697 L., Cai, X., Zhang, H., Yang, F., Wang, H., Yu, J. Z., Lau, A. K., He, L., Huang, X., Duan, L.,
698 Ding, A., Xue, L., Gao, J., Liu, B., and Zhu, T.: Ammonia emission control in China would

https://doi.org/10.5194/egusphere-2026-609
Preprint. Discussion started: 16 February 2026

mitigate haze pollution and nitrogen deposition, but worsen acid rain. Proc. Natl. Acad. Sci., 116(16), 7760–7765, https://doi.org/10.1073/pnas.1814880116, 2019.

Liu, M., Liu, Z., Wang, J., Chen, W., Feng, T., Pan, T., Yuan, B., Huang, S., Shao, M., Hu, M., Wang, X., and Hu, W.: The variation, source, and environmental impact of chloride across China: summarized field results based on the aerosol mass spectrometer (AMS). J. Geophys. Res.: Atmos., 130(11), e2024JD043275, https://doi.org/10.1029/2024JD043275, 2025.

Liu, P., Zhao, X., Zhang, C., Chen, H., Wang, J., Xue, L., Chen, J., and Mu, Y.: Fine particle pH and its influencing factors during summer at Mt. Tai: comparison between mountain and urban sites. Atmos. Environ., 261, 118607, https://doi.org/10.1016/j.atmosenv.2021.118607, 2021.

Liu, Y., Guo, X., Zhang, Y., Cao, Y., Jiang, Y., Qi, W., Shen, M., Li, L., Wang, Q., Dai, W., and Li, J.: Chemical characteristics of wintertime $PM_{2.5}$ in background region of northwest China during urban emission reduction. Iscience, 28(10), 113528, https://doi.org/10.1016/j.isci.2025.113528, 2025.

Mao, I., Lin, C, Lin, C., Chen, Y., Sung, F., and Chen, M.: Exposure of acid aerosol for schoolchildren in metropolitan Taipei. Atmos. Environ., 43(35), 5622–5629, https://doi.org/10.1016/j.atmosenv.2009.07.054, 2009.

Mao, M., Rao, L., Jiang, H., He, S., and Zhang, X.: Air pollutants in metropolises of eastern coastal China. Int. J. Environ. Res. Public Health, 19(22), 15332, https://doi.org/10.3390/ijerph192215332, 2022.

Meng, Z., Xu, X., Lin, W., Ge, B., Xie, Y., Song, B., Jia, S., Zhang, R., Peng, W., Wang, Y., Cheng, H., Yang, W., and Zhao, H.: Role of ambient ammonia in particulate ammonium formation at a rural site in the north China plain. Atmos. Chem. Phys., 18(1), 167–184, https://doi.org/10.5194/acp-18-167-2018, 2018.

Nah, T., Lam, Y. H., Yang, J., and Yang, L.: Long-term trends and sensitivities of $PM_{2.5}$ pH and aerosol liquid water to chemical composition changes and meteorological parameters in Hong Kong, south China: insights from 10-year records from three urban sites. Atmos. Environ., 302, 119725, https://doi.org/10.1016/j.atmosenv.2023.119725, 2023.

Nenes, A., Pandis, S. N., and Pilinis, C.: ISORROPIA: A new thermodynamic equilibrium

https://doi.org/10.5194/egusphere-2026-609
Preprint. Discussion started: 16 February 2026

model for multiphase multicomponent inorganic aerosols. Aquat. Geochem., 4, 123–152, https://doi.org/10.1023/A:1009604003981, 1998.

Niu, X., Cao, J., Shen, Z., Ho, S. S. H., Tie, X., Zhao, S., Xu, H., Zhang, T., and Huang, R.: $PM_{2.5}$ from the Guanzhong Plain: chemical composition and implications for emission reductions. Atmos. Environ., 147, 458–469, https://doi.org/10.1016/j.atmosenv.2016.10.029, 2016.

Paglione, M., Decesari, S., Rinaldi, M., Tarozzi, L., Manarini, F., Gilardoni, S., Facchini, M. C., Fuzzi, S., Bacco, D., Trentini, A., Pandis, S. N., and Nenes, A.: Historical changes in seasonal aerosol acidity in the po valley (Italy) as inferred from fog water and aerosol measurements. Environ. Sci. Technol., 55(11), 7307–7315, https://doi.org/10.1021/acs.est.1c00651, 2021.

Pye, H., Nenes, A., Alexander, B., Ault, A., Barth, M., Clegg, S., Collett Jr., J. L., Fahey, K., Hennigan, C., Herrmann, H., Kanakidou, M., Kelly, J., Ku, I., McNeill, V., Riemer, N., Schaefer, T., Shi, G., Tilgner, A., Walker, J., Wang, T., Weber, R., Xing, J., Zaveri, R., and Zuend, A.: The acidity of atmospheric particles and clouds. Atmos. Chem. Phys., 20(8), 4809–4888, https://doi.org/10.5194/acp-20-4809-2020, 2020.

Rengarajan, R., Sudheer, A., and Sarin, M.: Aerosol acidity and secondary organic aerosol formation during wintertime over urban environment in western India. Atmos. Environ., 45(11), 1940–1945, https://doi.org/10.1016/j.atmosenv.2011.01.026, 2011.

Saraswati, Sharma, S., Saxena, M., and Mandal, T.: Characteristics of gaseous and particulate ammonia and their role in the formation of secondary inorganic particulate matter at Delhi, India. Atmos. Res., 218, 34–49, https://doi.org/10.1016/j.atmosres.2018.11.010, 2019.

Shah, V., Jaeglé, L., Thornton, J., Lopez-Hilfiker, F., Lee, B., Schroder, J., Campuzano-Jost, P., Jimenez, J., Guo, H., Sullivan, A., Weber, R., Green, J., Fiddler, M., Bililign, S., Campos, T., Stell, M., Weinheimer, A., Montzka, D., and Brown, S.: Chemical feedbacks weaken the wintertime response of particulate sulfate and nitrate to emissions reductions over the eastern United States. Proc. Natl. Acad. Sci., 115(32), 8110–8115, https://doi.org/10.1073/pnas.1803295115, 2018.

Shen, M., Li, J., Liu, Y., Dai, W., Wang, G., Qi, W., Chen, Y., Guo, X., Zhang, Y., Li, L., Cao, Y., Feng, Q., Su, H., and Cao, J.: Comparison of acidity and chemical composition of

https://doi.org/10.5194/egusphere-2026-609
Preprint. Discussion started: 16 February 2026

summertime cloud water and aerosol at an alpine site in northwest China: Implications for the neutral property of clouds in the free troposphere. Sci. Total Environ., 925, 171775, https://doi.org/10.1016/j.scitotenv.2024.171775, 2024.

Shen, Z., Li, L., Du, N., Zhang, T., Cao, J., Li, Xu., and Zhu, C.: Mass concentration of atmospheric fine particles and characteristics of water-soluble components in Xi'an in spring. Ecol. Environ. Sci., 16(4), 1193–1198, https://doi.org/10.16258/j.cnki.1674-5906.2007.04.024, 2007.

Shi, G., Xu, J., Peng, X., Xiao, Z., Chen, K., Tian, Y., Guan, X., Feng, Y., Yu, H., Nenes, A., and Russell, A.: pH of aerosols in a polluted atmosphere: source contributions to highly acidic aerosol. Environ. Sci. Technol., 51(8), 4289–4296, https://doi.org/10.1021/acs.est.6b05736, 2017.

Shi, G., Xu, J., Shi, X., Liu, B., Bi, X., Xiao, Z., Chen, K., Wen, J., Dong, S., Tian, Y., Feng, Y., Yu, H., Song, S., Zhao, Q., Gao, J., and Russell, A. G.: Aerosol pH dynamics during haze periods in an urban environment in China: use of detailed, hourly, speciated observations to study the role of ammonia availability and secondary aerosol formation and urban environment. J. Geophys. Res.: Atmos., 124(16), 9730–9742, https://doi.org/10.1029/2018JD029976, 2019.

Shi, Z., Bonneville, S., Krom, M. D., Carslaw, K. S., Jickells, T. D., Baker, A. R., and Benning, L. G.: Iron dissolution kinetics of mineral dust at low pH during simulated atmospheric processing. Atmos. Chem. Phys., 11(3), 995–1007, https://doi.org/10.5194/acp-11-995-2011, 2011.

Su, J., Zhao, P., Ge, S., and Ding, J.: Aerosol liquid water content of PM2.5 and its influencing factors in Beijing, China. Sci. Total Environ., 839, 156342, https://doi.org/10.1016/j.scitotenv.2022.156342, 2022.

Sun, Y., Wang, Z., Fu, P., Yang, T., Jiang, Q., Dong, H., Li, J., and Jia, J.: Aerosol composition, sources and processes during wintertime in Beijing, China. Atmos. Chem. Phys., 13(9), 4577–4592, https://doi.org/10.5194/acp-13-4577-2013, 2013.

Tan, T., Hu, M., Li, M., Guo, Q., Wu, Y., Fang, X., Gu, F., Wang, Y., and Wu, Z.: New insight into $PM_{2.5}$ pollution patterns in Beijing based on one-year measurement of chemical compositions. Sci. Total Environ., 621, 734–743,

https://doi.org/10.5194/egusphere-2026-609
Preprint. Discussion started: 16 February 2026

https://doi.org/10.1016/j.scitotenv.2017.11.208, 2018.

Tang, I.: Chemical and size effects of hygroscopic aerosols on light scattering coefficients. J. Geophys. Res.: Atmos., 101(D14), 19245–19250, https://doi.org/10.1029/96JD03003, 1996.

Tao, J., Wu, Y., Deng, Y., Hu, B., and Zhou, Z.: Thermodynamic regulation of aerosol pH by temperature and humidity: the role of gas-particle partitioning of semi-volatile inorganic species in a subtropical region. Environ. Res., 286(1), 122727, https://doi.org/10.1016/j.envres.2025.122727, 2025.

Tao, Y. and Murphy, J. G.: The sensitivity of $PM_{2.5}$ acidity to meteorological parameters and chemical composition changes: 10-year records from six Canadian monitoring sites. Atmos. Chem. Phys., 19(14), 9309–9320, https://doi.org/10.5194/acp-19-9309-2019, 2019.

Wang, G., Zhang, R., Gomez, M., Yang, L., Levy Zamora, M., Hu, M., Lin, Y., Peng, J., Guo, S., Meng, J., Li, J., Cheng, C., Hu, T., Ren, Y., Wang, Y., Gao, J., Cao, J., An, Z., Zhou, W., Li, G., Wang, J., Tian, P., Marrero-Ortiz, W., Secrest, J., Du, Z., Zheng, J., Shang, D., Zeng, L., Shao, M., Wang, W., Huang, Y., Wang, Y., Zhu, Y., Li, Y., Hu, J., Pan, B., Cai, L., Cheng, Y., Ji, Y., Zhang, F., Rosenfeld, D., Liss, P., Duce, R., Kolb, C., and Molina, M.: Persistent sulfate formation from London fog to Chinese haze. Proc. Natl. Acad. Sci., 113(48), 13630–13635, https://doi.org/10.1073/pnas.1616540113, 2016.

Wang, Q., Guo, Xiao., Shen, M., Liu, Y., Zhang, Y., Li, L., Qi, W., Cao, Y., Li, S., Dong, Z., and Dai, W.:Measurement report: quantitative analysis of aerosol acidity and its driving factors in guanzhong area, northwest China. Zenodo [data set], https://zenodo.org/records/18455742, 2026.

Wang, Z., Wang, R., Wang, J., Wang, Y., McPherson Donahue, N., Tang, R., Dong, Z., Li, X., Wang, L., Han, Y., and Cao, J.: The seasonal variation, characteristics and secondary generation of $PM_{2.5}$ in Xi'an, China, especially during pollution events. Environ. Res., 212, 113388, https://doi.org/10.1016/j.envres.2022.113388, 2022.

Wei, Y., Wang, S., Jiang, N., Zhang, R., and Hao, Q.: Comparative multi-model study of $PM_{2.5}$ acidity trend changes in ammonia-rich regions in winter: based on a new ammonia concentration assessment method. J. Hazard. Mater., 458, 131970, https://doi.org/10.1016/j.jhazmat.2023.131970, 2023.

Wu, C., Wang, G., Li, J., Li, J.J., Cao, C., Ge, S., Xie, Y., Chen, J., Li, X., Xue, G., Wang, X.,

https://doi.org/10.5194/egusphere-2026-609
Preprint. Discussion started: 16 February 2026

Zhao, Z., and Cao, F.: The characteristics of atmospheric brown carbon in Xi'an, inland China: sources, size distributions and optical properties. Atmos. Chem. Phys., 20(4), 2017–2030, https://doi.org/10.5194/acp-20-2017-2020,2020.

Xie, Y., Lu, H., Yi, A., Zhang, Z., Zheng, N., Fang, X., and Xiao, H.: Characterization and source analysis of water–soluble ions in $PM_{2.5}$ at a background site in central China. Atmos. Res., 239, 104881, https://doi.org/10.1016/j.atmosres.2020.104881, 2020.

Xu, K., Yin, L., Chen, Q., Liao, D., Ji, X., Zhang, K., Wu, Y., Xu, L., Li, M., Fan, X., Zhang, F., Huang, Z., Chen, J., and Hong, Y.: Quantitative analysis of influencing factors to aerosol pH and its responses to $PM_{2.5}$ and O_3 pollution in a coastal city. J. Environ. Sci., 151, 284–297, https://doi.org/10.1016/j.jes.2024.03.044, 2025.

Zhang, B., Shen, H., Liu, P., Guo, H., Hu, Y., Chen, Y., Xie, S., Xi, Z., Skipper, T., and Russell, A.: Significant contrasts in aerosol acidity between China and the United States. Atmos. Chem. Phys., 21(10), 8341–8356, https://doi.org/10.5194/acp-21-8341-2021, 2021.

Zhang, Q., Shen, Z., Lei, Y., Zhang, T., and Zhang, R.: Optical properties and source identification of black carbon and brown carbon: Comparison of winter and summer haze episodes in Xi'an, northwest China. Environ Sci: Processes Impacts, 21(12), 2058–2069, 2019.

Zhang, R., Han, Y., Shi, A., Sun, X., Yan, X., Huang, Y., and Wang, Y.: Characteristics of ambient ammonia and its effects on particulate ammonium in winter of urban Beijing, China. Environ. Sci. Pollut. Res., 28(44), 62828–62838, https://doi.org/10.1007/s11356-021-14108-w, 2021.

Zhang, T., Shen, Z., Su, H., Liu, S., Zhou, J., Zhao, Z., Wang, Q., Prévôt, A. S. H., and Cao, J. J.: Effects of aerosol water content on the formation of secondary inorganic aerosol during a winter heavy $PM_{2.5}$ pollution episode in Xi'an, China. Atmos. Environ., 252, 118304, https://doi.org/10.1016/j.atmosenv.2021.118304, 2021.

Zhang, Y., Cai, J., Wang, S., He, K., and Zheng, M.: Review of receptor-based source apportionment research of fine particulate matter and its challenges in China. Sci. Total Environ., 586, 917–929, https://doi.org/10.1016/j.scitotenv.2017.02.071, 2017.

Zheng, G., Su, H., Wang, S., Andreae, M., Pöschl, U., and Cheng, Y.: Multiphase buffer theory explains contrasts in atmospheric aerosol acidity. Science, 369(6509), 1374–1377,

https://doi.org/10.5194/egusphere-2026-609
Preprint. Discussion started: 16 February 2026

https://doi.org/10.1126/science.aba3719, 2020.

Zheng, G., Su, H., and Cheng, Y.: Role of carbon dioxide, ammonia, and organic acids in buffering atmospheric acidity: The distinct contribution in clouds and aerosols. Environ. Sci. Technol., 57(34), 12571–12582, https://doi.org/10.1021/acs.est.2c09851, 2023.

Zhou, M., Zheng, G., Wang, H., Qiao, L., Zhu, S., Huang, D., An, J., Lou, S., Tao, S., Wang, Q., Yan, R., Ma, Y., Chen, C., Cheng, Y., Su, H., and Huang, C.: Long-term trends and drivers of aerosol pH in eastern China. Atmos. Chem. Phys., 22(20), 13833–13844, https://doi.org/10.5194/acp-22-13833-2022, 2022.

https://doi.org/10.5194/egusphere-2026-609
Preprint. Discussion started: 16 February 2026

Table 1 Multiple linear regression results between NHR and its drivers (major particulate ions and meteorological factos) in each season.

	Annual	Winter	Spring	Summer	Autumn
$PM_{2.5}$ (μg m^{-3})	65.3 ± 61.8	93.5 ± 41.7	61.4 ± 40.8	33.3 ± 13.7	43.1 ± 25.1
PM_{10} (μg m^{-3})	97.5 ± 66.3	146.0 ± 61.1	87.7 ± 66.6	39.3 ± 14.3	94.2 ± 49.1
T (K)	289.3 ± 10.1	278.2 ± 4.2	291.1 ± 5.3	302.0 ± 4.0	290.3 ± 5.1
RH (%)	66.5 ± 20.2	65.5 ± 20.9	62.2 ± 19.8	61.2 ± 19.1	80.0 ± 14.8
WS (m s^{-1})	0.7 ± 0.3	0.7 ± 0.2	0.8 ± 0.3	0.9 ± 0.3	0.6 ± 0.2
SO_2 (μg m^{-3})	8.9 ± 4.6	10.0 ± 4.5	4.9 ± 2.0	8.6 ± 3.4	11.9 ± 5.0
CO (mg m^{-3})	0.7 ± 0.4	1.1 ± 0.5	0.5 ± 0.1	0.4 ± 0.1	0.6 ± 0.2
NO_2 (μg m^{-3})	25.9 ± 15.1	37.4 ± 13.2	25.0 ± 8.4	9.8 ± 4.5	26.4 ± 14.4
O_3 (μg m^{-3})	99.6 ± 50.1	67.8 ± 33.2	109.5 ± 40.2	150.2 ± 43.2	83.4 ± 39.7
WSIIs(μg m^{-3})	24.5 ± 20.5	39.5 ± 22.0	18.6 ± 12.9	8.5 ± 4.2	19.8 ± 15.9
SNA (μg m^{-3})	21.8 ± 19.4	35.5 ±21.1	16.1 ± 12.3	7.0 ± 3.7	18.1 ± 15.5
SO_4^{2-} (μg m^{-3})	5.1 ± 3.7	7.3 ± 4.7	4.1 ± 1.7	3.4 ± 2.1	4.4 ± 3.1
NO_3^- (μg m^{-3})	8.8 ± 10.8	16.3 ± 11.9	6.1 ± 7.0	1.0 ± 1.2	8.7 ± 10.8
NH_4^+ (μg m^{-3})	4.0 ± 4.7	7.3 ± 5.7	2.4 ± 2.6	1.1 ± 0.8	3.8 ± 4.1
Cl^- (μg m^{-3})	0.5 ± 0.7	1.1 ± 0.8	0.3 ± 0.2	0.1 ± 0.1	0.3 ± 0.3
Ca^{2+} (μg/m^3)	1.4 ± 1.6	1.8 ± 1.8	1.9 ± 1.6	0.8 ± 0.6	0.6 ± 0.3
K^+ (μg m^{-3})	0.3 ± 0.4	0.6 ± 0.4	0.2 ± 0.1	0.1 ± 0.1	0.2 ± 0.2
Mg^{2+} (μg m^{-3})	0.1 ± 0.1	0.2 ± 0.1	0.2 ± 0.1	0.1 ± 0.1	0.1 ± 0.1
Na^+ (μg/m^3)	0.7 ± 0.4	0.9 ± 0.5	0.7 ± 0.2	0.6 ± 0.2	0.6 ± 0.1
NH_3 (μg m^{-3})	12.8 ± 10.3	22.6 ± 10.0	5.9 ± 4.3	12.1 ± 5.5	4.5 ± 3.9
NH_x (μg m^{-3})	16.7 ± 14.1	29.7 ± 15.1	8.3 ± 6.8	13.2 ± 6.3	8.4 ± 7.9
NHR	0.2 ± 0.1	0.2 ± 0.1	0.2 ± 0.1	0.1 ± 0.1	0.4 ± 0.1

Table 2 Multiple linear regression results between NHR and its drivers (major particulate ions and meteorological factos) in each season.

Season	Prediction Equation	R	Sig.
Winter	$NHR = 1.204 - 0.003SO_4^{2-} + 0.006NO_3^- + 0.023K^+ + 0.328Mg^{2+} - 0.017Ca^{2+} - 0.004T + 0.001RH$	0.88	$P < 0.01$
Spring	$NHR = 0.533 + 0.006SO_4^{2-} + 0.005NO_3^- - 0.018K^+ - 0.065Mg^{2+} - 0.017Ca^{2+} - 0.001T - 0.009RH$	0.83	
Summer	$NHR = -1.389 + 0.007SO_4^{2-} + 0.006NO_3^- + 0.01K^+ + 0.021Mg^{2+} - 0.003Ca^{2+} + 0.005T - 0.066RH$	0.82	
Autumn	$NHR = 0.656 + 0.006SO_4^{2-} + 0.003NO_3^- - 0.003K^+ + 0.064Mg^{2+} - 0.040Ca^{2+} - 0.001T + 0.012RH$	0.86	

https://doi.org/10.5194/egusphere-2026-609
Preprint. Discussion started: 16 February 2026

868

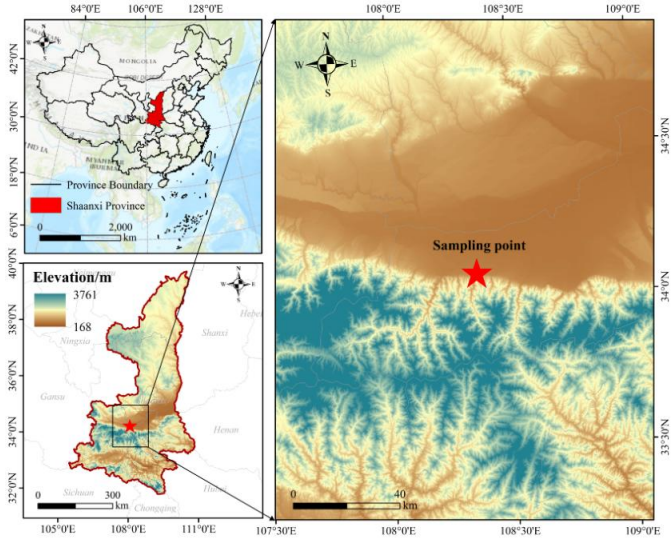

869

870 **Fig.1 Locations of monitoring stations in Qinling**

871

872

https://doi.org/10.5194/egusphere-2026-609
Preprint. Discussion started: 16 February 2026

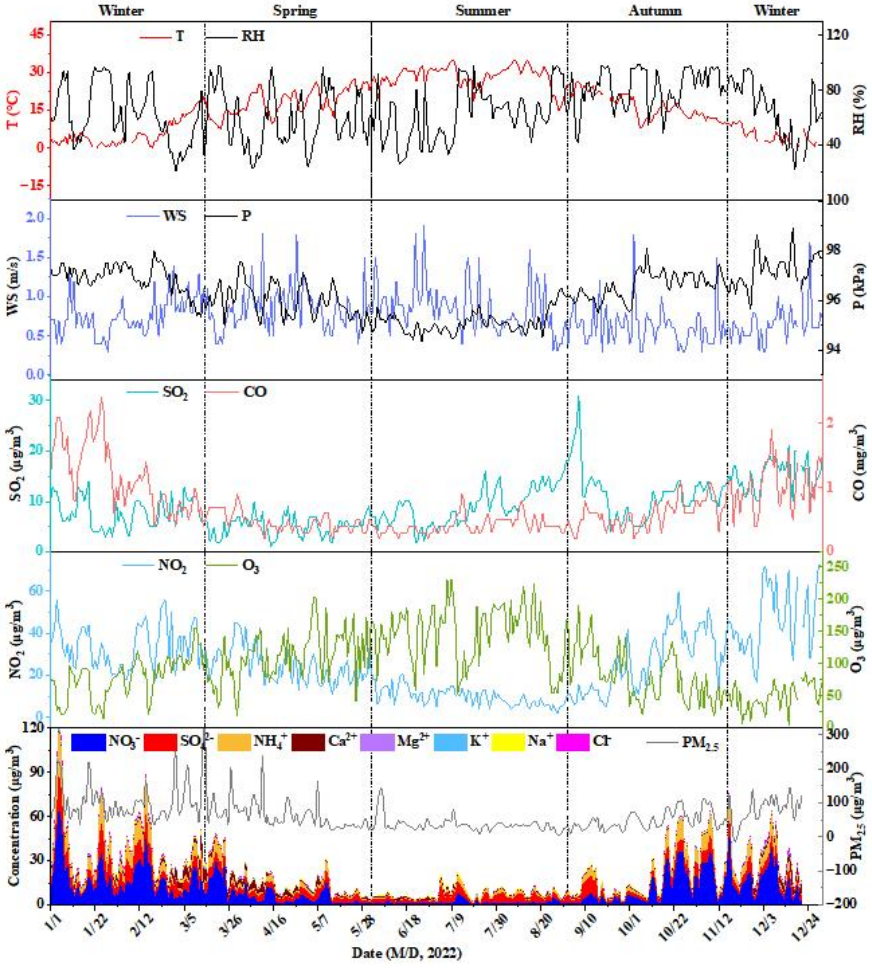

873

874 **Fig. 2 The time series data for $PM_{2.5}$ mass concentrations, criteria air pollutants (SO_2, CO,**

875 **NO_2, and O_3-8h), and meteorological parameters (T, RH, WS, and AP).**

876

https://doi.org/10.5194/egusphere-2026-609
Preprint. Discussion started: 16 February 2026

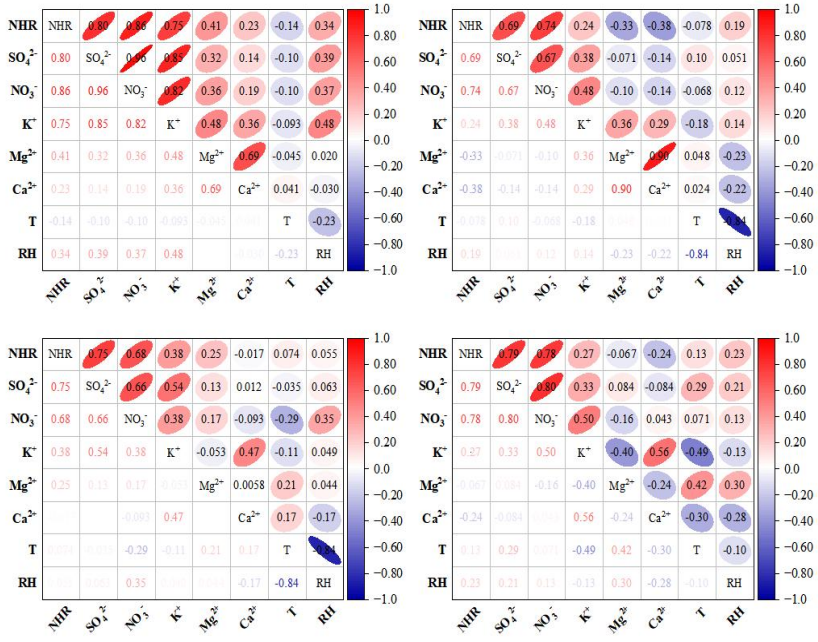

877

878 **Fig. 3 Pearson correlation among various factors**

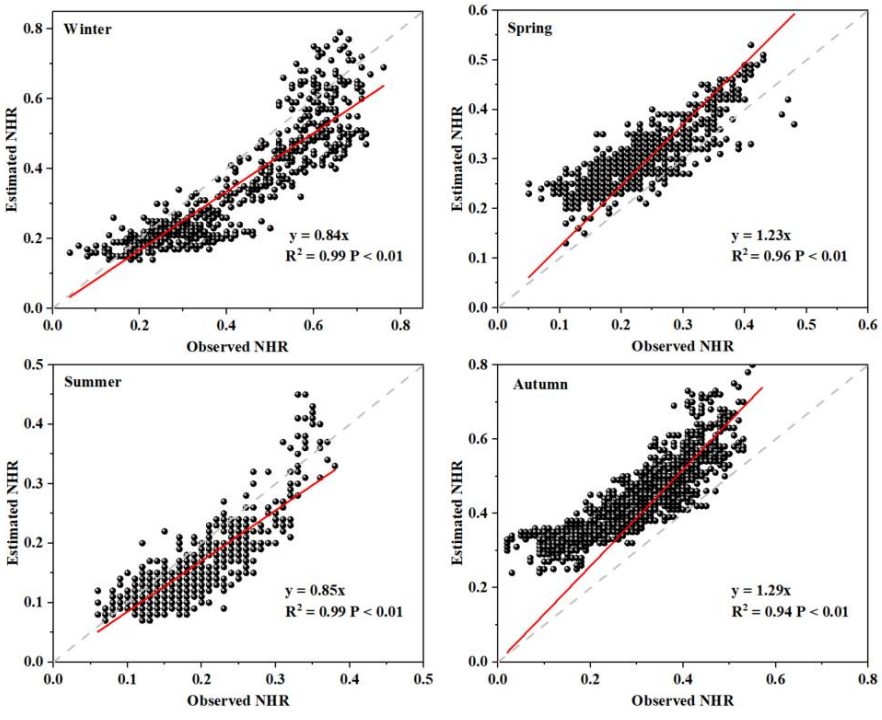

879

880 **Fig. 4 Correlation between estimated and observed daily average values of NHR.**

https://doi.org/10.5194/egusphere-2026-609
Preprint. Discussion started: 16 February 2026

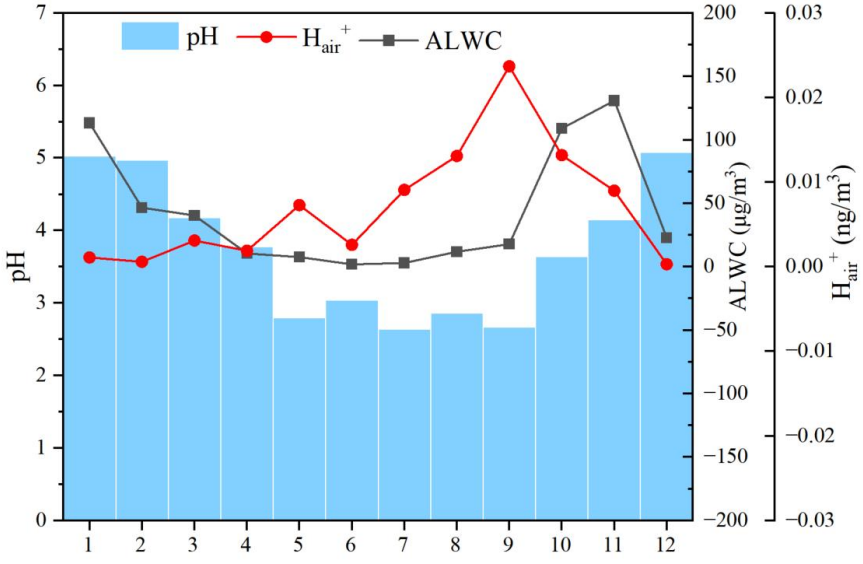

881

882 **Fig.5 Monthly average aerosol pH, ALWC and H_{air}^{+} changes**

883

https://doi.org/10.5194/egusphere-2026-609
Preprint. Discussion started: 16 February 2026

884

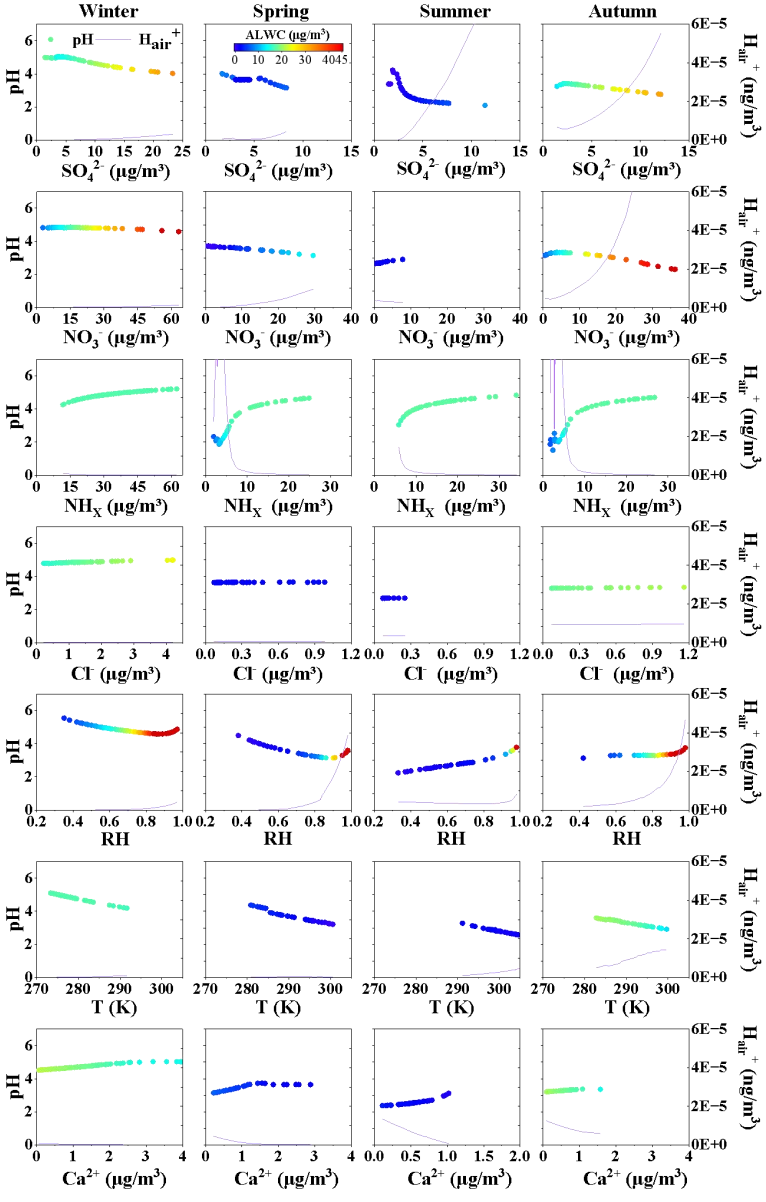

885

886 **Fig. 6 Sensitivity analysis of influencing factors**

887

888

https://doi.org/10.5194/egusphere-2026-609
Preprint. Discussion started: 16 February 2026

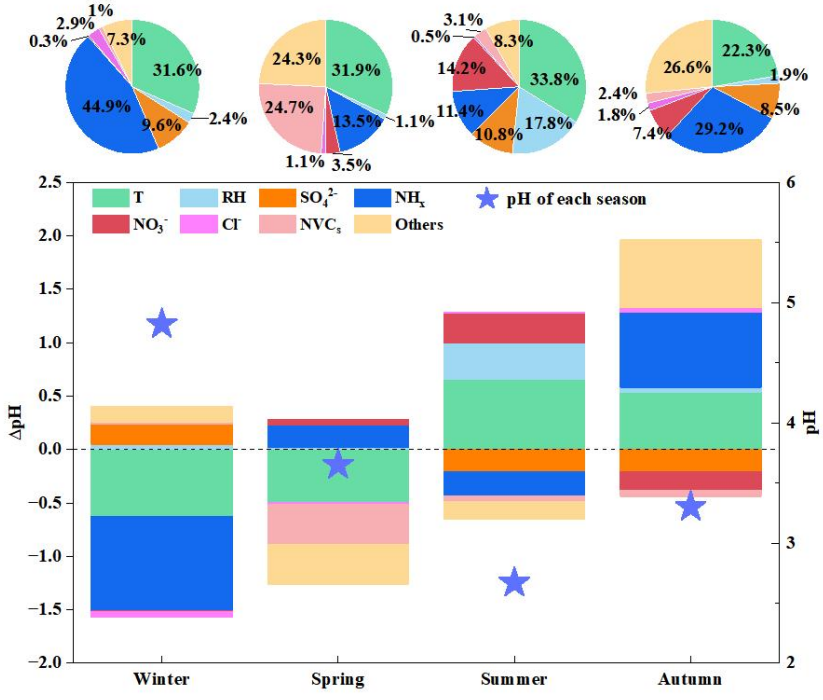

Fig. 7 The contribution of various influencing factors to the seasonal pH. The asterisk represents the pH of aerosols in each season. The pie chart shows the relative contributions of various influencing factors to the seasonal pH (absolute values of pH was taken for pie chart).